Error Probability Bounds for Balanced Binary Relay Trees

Zhenliang Zhang, *Student Member, IEEE*, Ali Pezeshki, *Member, IEEE*, William Moran, *Member, IEEE*, Stephen D. Howard, *Member, IEEE*, and Edwin K. P. Chong, *Fellow, IEEE*

***Abstract*—We study the detection error probability associated with a balanced binary relay tree, where the leaves of the tree correspond to N identical and independent sensors. The root of the tree represents a fusion center that makes the overall detection decision. Each of the other nodes in the tree is a relay node that combines two binary messages to form a single output binary message. Only the leaves are sensors. In this way, the information from the sensors is aggregated into the fusion center via the relay nodes. In this context, we describe the evolution of the Type I and Type II error probabilities of the binary data as it propagates from the leaves toward the root. Tight upper and lower bounds for the total error probability at the fusion center as functions of N are derived. These characterize how fast the total error probability converges to 0 with respect to N, even if the individual sensors have error probabilities that converge to $1/2$.**

***Index Terms*—Binary relay tree, decay rate, decentralized detection, distributed detection, dynamic system, error probability, hypothesis testing, information fusion, invariant region, sensor network.**

I. Introduction

CONSIDER a hypothesis testing problem under two scenarios: *centralized* and *decentralized*. Under the centralized network scenario, all sensors send their raw measurements to the fusion center, which makes a decision based on these measurements. In the decentralized network introduced in [1], sensors send summaries of their measurements and observations to the fusion center. The fusion center then makes a decision. In a decentralized network, information is summarized into smaller messages. Evidently, the decentralized network cannot perform better than the centralized network. It gains because of its limited use of resources and bandwidth; through transmission of summarized information, it is more practical and efficient.

The decentralized network in [1] involves the parallel architecture, also known as the *star* architecture [1]–[17], [33], in which all sensors directly connect to the fusion center. A typical result is that under the assumption of (conditionally) independence of the sensor observations, the decay rate of the error probability in the parallel architecture is exponential [6].

Several different sensor topologies have been studied under the assumption of conditional independence. The first configuration for such a fusion network considered was the tandem network [18]–[22], [33], in which each nonleaf node combines the information from its own sensor with the message it has received from the node at one level down, which is then transmitted to the node at the next level up. The decay rate of the error probability in this case is subexponential [22]. Specifically, as the number of sensors N goes to infinity, the exponent of the error probability is dominated by N^d asymptotically for all $d > 1/2$ [20]. This sensor network represents a situation where the length of the network is the longest possible among all networks with N leaf nodes.

The asymptotic performance of single-rooted tree network with bounded height is discussed in [23]–[31], [33]. Even though the error probability in the parallel configuration decreases exponentially, in a practical implementation, the resources consumed in having each sensor transmit directly to the fusion center might be regarded as excessive. Energy consumption can be reduced by setting up a directed tree, rooted at the fusion center. In this tree structure, measurements are summarized by leaf sensor nodes and sent to their parent nodes, each of which fuses all the messages it receives with its own measurement (if any) and then forwards the new message to its parent node at the next level. This process takes place throughout the tree culminating in the fusion center, where a final decision is made. For bounded-height tree configuration under the Neyman–Pearson criterion, the optimal error exponent is as good as that of the parallel configuration under certain conditions. For example, for a bounded-height tree network with $\lim_{\tau_N \to \infty} \ell_N/\tau_N = 1$, where τ_N denotes the total number of nodes and ℓ_N denotes the number of leaf nodes, the optimal error exponent is the same as that of the parallel configuration [24], [26]. For bounded-height tree configuration under the Bayesian criterion, the error probability decays exponentially fast to 0 with an error exponent which is worse than the one associated with the parallel configuration [27].

The variation of detection performance with increasing tree height is still largely unexplored. If only the leaf nodes have

Manuscript received April 26, 2011; revised October 19, 2011; accepted December 14, 2011. Date of publication February 10, 2012; date of current version May 15, 2012. This work was supported in part by the Air Force Office of Scientific Research under Contract FA9550-09-1-0518 and in part by the National Science Foundation under Grants ECCS-0700559, CCF-0916314, and CCF-1018472. The material in this paper was presented in part at the Joint 50th IEEE Conference on Decision and Control and European Control Conference, Orlando, FL, December 2011.

Z. Zhang, A. Pezeshki, and E. K. P. Chong are with the Department of Electrical and Computer Engineering, Colorado State University, Fort Collins, CO 80523-1373 USA (e-mail: zhenliang.zhang@colostate.edu; ali.pezeshki@colostate.edu; edwin.chong@colostate.edu).

W. Moran is with the Department of Electrical and Electronic Engineering, The University of Melbourne, Melbourne, VIC 3010, Australia (e-mail: wmoran@unimelb.edu.au).

S. D. Howard is with the Defence Science and Technology Organisation, Edinburgh, SA 5111, Australia (e-mail: sdhoward@unimelb.edu.au).

Communicated by G. Moustakides, Associate Editor for Detection and Estimation.

Color versions of one or more of the figures in this paper are available online at http://ieeexplore.ieee.org.

Digital Object Identifier 10.1109/TIT.2012.2187323

sensors making observations, and all other nodes simply fuse the messages received and forward the new messages to their parents, the tree network is known as a *relay tree*. The balanced binary relay tree has been addressed in [32], in which it is assumed that the leaf nodes are independent sensors with identical Type I error probability (also known as the probability of false alarm, denoted by α_0) and identical Type II error probability (also known as the probability of missed detection, denoted by β_0). It is shown there that if the sensor error probabilities satisfy the condition $\alpha_0 + \beta_0 < 1$, then both the Type I and Type II error probabilities at the fusion center converge to 0 as the N goes to infinity. If $\alpha_0 + \beta_0 > 1$, then both the Type I and Type II error probabilities converge to 1, which means that if we flip the decision at the fusion center, then the Type I and Type II error probabilities converge to 0. Because of this symmetry, it suffices to consider the case where $\alpha_0 + \beta_0 < 1$. If $\alpha_0 + \beta_0 = 1$, then the Type I and II error probabilities add up to 1 at each node of the tree. In consequence, this case is not of interest.

We consider the balanced binary relay tree configuration in this paper and describe the precise evolution of the Type I and Type II error probabilities in this case. In addition, we provide upper and lower bounds for the total error probability at the fusion center as functions of N. These characterize the decay rate of the total error probability. We also show that the total error probability converges to 0 under certain condition even if the sensors are asymptotically crummy, that is, $\alpha_0 + \beta_0 \to 1$.

The rest of this paper is organized as follows. In Section II, we formulate the decentralized detection problem in the setting of balanced binary relay trees. In Section III, we discuss the evolution of the Type I and Type II error probabilities. In Section IV, we derive upper and lower bounds for the total error probability at the fusion center as functions of N. In Section V, we discuss some corollaries focusing on the asymptotic regime as $N \to \infty$. Finally, Section VI contains the concluding remarks.

II. Problem Formulation

We consider the problem of binary hypothesis testing between H_0 and H_1 in a balanced binary relay tree. Leaf nodes are sensors undertaking initial and independent detections of the same event in a scene. These measurements are summarized into binary messages and forwarded to nodes at the next level. Each nonleaf node with the exception of the root, the fusion center, is a relay node, which fuses two binary messages into one new binary message and forwards the new binary message to its parent node. This process takes place at each node culminating in the fusion center, at which the final decision is made based on the information received. Only the leaves are sensors in this tree architecture.

In this configuration, as shown in Fig. 1, the closest sensor to the fusion center is as far as it could be, in terms of the number of arcs in the path to the root. In this sense, this configuration is the worst case among all relay trees with N sensors. Moreover, in contrast to the configuration in [24] and [26] discussed earlier, in our balanced binary tree we have $\lim_{\tau_N \to \infty} \ell_N / \tau_N = 1/2$ (as opposed to 1 in [24] and [26]). Hence, the number of times that information is aggregated is essentially as large as the number of measurements (cf., [24] and [26], in which the number of measurements dominates the number of fusions). In addition,

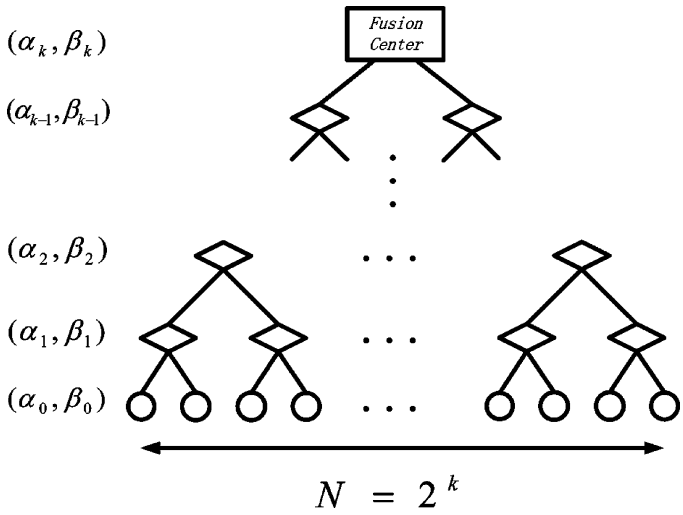

Fig. 1. Balanced binary relay tree with height k. Circles represent sensors making measurements. Diamonds represent relay nodes which fuse binary messages. The rectangle at the root represents the fusion center making an overall decision.

the height of the tree is $\log N$, which grows as the number of sensors increases. (Throughout this paper, log stands for the binary logarithm.)

We assume that all sensors are independent given each hypothesis, and that all sensors have identical Type I error probability α_0 and identical Type II error probability β_0. We apply the likelihood-ratio test [34] with threshold 1 as the fusion rule at the relay nodes and at the fusion center. This fusion rule is locally (but not necessarily globally) optimal in the case of equally likely hypotheses H_0 and H_1; i.e., it minimizes the total error probability locally at each fusion node. In the case where the hypotheses are not equally likely, the locally optimal fusion rule has a different threshold value, which is the ratio of the two hypothesis probabilities. However, this complicates the analysis without bringing any additional insights. Therefore, for simplicity, we, henceforth, assume a threshold value of 1 in our analysis. We are interested in following questions.

1) What are these Type I and Type II error probabilities as functions of N?
2) Will they converge to 0 at the fusion center?
3) If yes, how fast will they converge with respect to N?

Fusion at a single node receiving information from the two immediate child nodes where these have identical Type I error probabilities α and identical Type II error probabilities β provides a detection with Type I and Type II error probabilities denoted by (α', β'), and given by [32]:

$$(\alpha', \beta') = f(\alpha, \beta) := \begin{cases} (1-(1-\alpha)^2, \beta^2), & \alpha \le \beta \\ (\alpha^2, 1-(1-\beta)^2), & \alpha > \beta. \end{cases} \quad (1)$$

Evidently, as all sensors have the same error probability pair (α_0, β_0), all relay nodes at level 1 will have the same error probability pair $(\alpha_1, \beta_1) = f(\alpha_0, \beta_0)$, and by recursion

$$(\alpha_{k+1}, \beta_{k+1}) = f(\alpha_k, \beta_k), \qquad k = 0, 1, \ldots \quad (2)$$

where (α_k, β_k) is the error probability pair of nodes at the kth level of the tree.

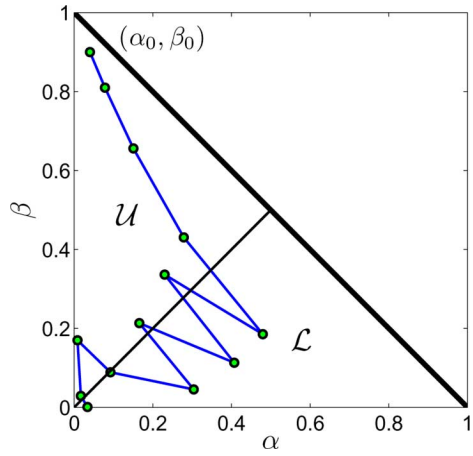

Fig. 2. Trajectory of the sequence $\{(\alpha_k, \beta_k)\}$ in the (α, β) plane.

The recursive relation (2) allows us to consider the pair of the Type I and II error probabilities as a discrete dynamic system. In [32], which focuses on the convergence issues for the total error probability, convergence was proved using Lyapunov methods. The analysis of the precise evolution of the sequence $\{(\alpha_k, \beta_k)\}$ and the total error probability decay rate remains open. In this paper, we will establish upper and lower bounds for the total error probability and deduce the precise decay rate of the total error probability.

To illustrate the ideas, consider first a single trajectory for the dynamic system given by (1), and starting at the initial state (α_0, β_0). This trajectory is shown in Fig. 2. It exhibits different behaviors depending on its distance from the $\beta = \alpha$ line. The trajectory approaches $\beta = \alpha$ very fast initially, but when (α_k, β_k) approaches within a certain neighborhood of the line $\beta = \alpha$, the next pair $(\alpha_{k+1}, \beta_{k+1})$ will appear on the other side of that line. In Section III, we will establish theorems that characterize the precise step-by-step behavior of the dynamic system (2). In Section IV, we derive upper and lower bounds for (twice) the total error probability P_N at the fusion center as functions of N. These bounds show that the convergence of the total error probability is subexponential. Specifically, the exponent of P_N is essentially $\sqrt{N}$ (cf., [24], [26], and [27], where the convergence of the total error probability is exponential in trees with bounded height; more precisely, under the Neyman–Pearson criterion, the optimal error exponent is the same as that of the parallel configuration if leaf nodes dominate; i.e., $\lim_{\tau_N \to \infty} \ell_N / \tau_N = 1$, but under the Bayesian criterion it is worse).

III. Evolution of the Type I and II Error Probabilities

Relation (1) is symmetric about both of the lines $\alpha + \beta = 1$ and $\beta = \alpha$. Therefore, it suffices to study the evolution of the dynamic system $\{(\alpha_k, \beta_k)\}$ only in the region bounded by $\alpha + \beta < 1$ and $\beta \geq \alpha$. We denote

$$\mathcal{U} := \{(\alpha, \beta) \geq 0 | \alpha + \beta < 1 \text{ and } \beta \geq \alpha\}$$

to be this triangular region. Similarly, define the complementary triangular region

$$\mathcal{L} := \{(\alpha, \beta) \geq 0 | \alpha + \beta < 1 \text{ and } \beta < \alpha\}.$$

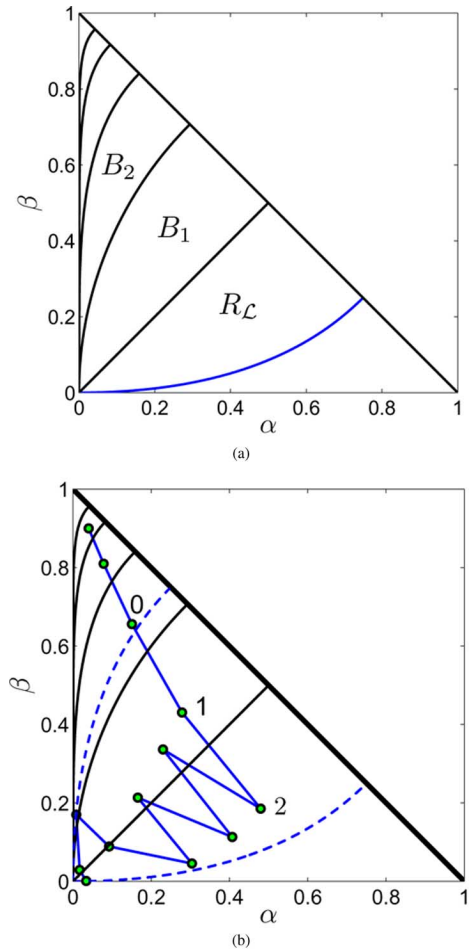

Fig. 3. (a) Regions B_1, B_2, and $R_{\mathcal{L}}$ in the (α, β) plane. (b) Trajectory in Fig. 2 superimposed on (a), where solid lines represent boundaries of B_m and dashed lines represent boundaries of R.

We denote the following region by B_1:

$$B_1 := \{(\alpha, \beta) \in \mathcal{U} | (1-\alpha)^2 + \beta^2 \leq 1\}.$$

If $(\alpha_k, \beta_k) \in B_1$, then the next pair $(\alpha_{k+1}, \beta_{k+1}) = f(\alpha_k, \beta_k)$ crosses the line $\beta = \alpha$ to the opposite side from (α_k, β_k). More precisely, if $(\alpha_k, \beta_k) \in \mathcal{U}$, then $(\alpha_k, \beta_k) \in B_1$ if and only if $(\alpha_{k+1}, \beta_{k+1}) = f(\alpha_k, \beta_k) \in \mathcal{L}$. In other words, B_1 is the *inverse image* of $\mathcal{L}$ under mapping f in $\mathcal{U}$. The set B_1 is shown in Fig. 3(a). Fig. 3(b) illustrates this behavior of the trajectory for the example in Fig. 2. For instance, as shown in Fig. 3(b), if the state is at point 1 in B_1, then it jumps to the next state point 2, on the other side of $\beta = \alpha$.

Denote the following region by B_2:

$$B_2 := \{(\alpha, \beta) \in \mathcal{U} | (1-\alpha)^2 + \beta^2 \geq 1 \text{ and } (1-\alpha)^4 + \beta^4 \leq 1\}.$$

It is easy to show that if $(\alpha_k, \beta_k) \in \mathcal{U}$, then $(\alpha_k, \beta_k) \in B_2$ if and only if $(\alpha_{k+1}, \beta_{k+1}) = f(\alpha_k, \beta_k) \in B_1$. In other words, B_2 is the inverse image of B_1 in $\mathcal{U}$ under mapping f. The behavior of f is illustrated in the movement from point 0 to point 1 in Fig. 3(b). The set B_2 is identified in Fig. 3(a), lying directly above B_1.

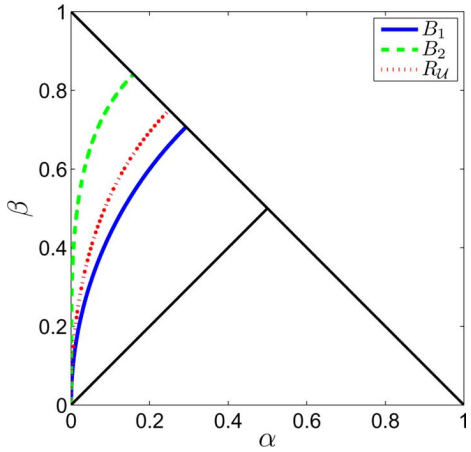

Fig. 4. Upper boundaries of B_1, B_2, and $R_{\mathcal{U}}$.

Now for an integer $m > 1$, recursively define B_m to be the inverse image of B_{m-1} under mapping f, denoted by B_m. It is easy to see that

$$B_m := \{(\alpha,\beta) \in \mathcal{U} | (1-\alpha)^{2^{(m-1)}} + \beta^{2^{(m-1)}} \geq 1 \text{ and } (1-\alpha)^{2^m} + \beta^{2^m} \leq 1\}.$$

Notice that $\mathcal{U} = \bigcup_{m=1}^{\infty} B_m$. Hence, for any $(\alpha_0,\beta_0) \in \mathcal{U}$, there exists m such that $(\alpha_0,\beta_0) \in B_m$. This gives a complete description of how the dynamics of the system behaves in the upper triangular region $\mathcal{U}$. For instance, if the initial pair (α_0,β_0) lies in B_m, then the system evolves in the order

$$B_m \to B_{m-1} \to \cdots \to B_2 \to B_1.$$

Therefore, the system will enter B_1 after $m-1$ levels of fusion; i.e., $(\alpha_{m-1},\beta_{m-1}) \in B_1$.

As the next stage, we consider the behavior of the system after it enters B_1. The *image* of B_1 under mapping f, denoted by $R_{\mathcal{L}}$, is [see Fig. 3(a)]

$$R_{\mathcal{L}} := \{(\alpha,\beta) \in \mathcal{L} | \sqrt{1-\alpha} + \sqrt{\beta} \geq 1\}.$$

We can define the reflection of B_m about the line $\beta = \alpha$ in the similar way for all m. Similarly, we denote by $R_{\mathcal{U}}$ the reflection of $R_{\mathcal{L}}$ about the line $\beta = \alpha$; i.e.,

$$R_{\mathcal{U}} := \{(\alpha,\beta) \in \mathcal{U} | \sqrt{1-\beta} + \sqrt{\alpha} \geq 1\}.$$

We denote the region $R_{\mathcal{U}} \cup R_{\mathcal{L}}$ by R. We will show that R is an *invariant region* in the sense that once the dynamic system enters R, it stays there. For example, as shown in Fig. 3(b), the system after point 1 stays inside R.

Proposition 1: If $(\alpha_{k_0},\beta_{k_0}) \in R$ for some k_0, then $(\alpha_k,\beta_k) \in R$ for all $k \geq k_0$.

Proof: First, we show that $B_1 \subset R_{\mathcal{U}} \subset B_1 \cup B_2$.

Notice that B_1, $R_{\mathcal{U}}$, and $B_1 \cup B_2$ share the same lower boundary $\beta = \alpha$. It suffices to show that the upper boundary of $R_{\mathcal{U}}$ lies between the upper boundary of B_2 and that of B_1 (see Fig. 4).

First, we show that the upper boundary of $R_{\mathcal{U}}$ lies above the upper boundary of B_1. We have

$$\begin{aligned} & 1-(1-\sqrt{\alpha})^2 \geq \sqrt{1-(1-\alpha)^2} \\ \Longleftrightarrow & 2\sqrt{\alpha} - \alpha \geq \sqrt{2\alpha - \alpha^2} \\ \Longleftrightarrow & \alpha^2 + \alpha - 2\alpha^{3/2} \geq 0 \end{aligned}$$

which holds for all α in $[0,1)$. Thus, $B_1 \subset R_{\mathcal{U}}$.

Now we prove that the upper boundary of $R_{\mathcal{U}}$ lies below that of B_2. We have

$$\begin{aligned} & (1-(1-\alpha)^4)^{1/4} \geq 1-(1-\sqrt{\alpha})^2 \\ \Longleftrightarrow & 1-(1-\alpha)^4 \geq (2\sqrt{\alpha}-\alpha)^4 \\ \Longleftrightarrow & -2(\sqrt{\alpha}-1)^2\alpha(-\alpha^{3/2} + \alpha(\sqrt{\alpha}-1) \\ & + 4\sqrt{\alpha}(\sqrt{\alpha}-1) + \alpha - 2) \geq 0 \end{aligned}$$

which holds for all α in $[0,1)$ as well. Hence, $R_{\mathcal{U}} \subset B_1 \cup B_2$.

Without loss of generality, we assume that $(\alpha_{k_0},\beta_{k_0}) \in R_{\mathcal{U}}$. It means that $(\alpha_{k_0},\beta_{k_0}) \in B_1$ or $(\alpha_{k_0},\beta_{k_0}) \in B_2 \cap R_{\mathcal{U}}$. If $(\alpha_{k_0},\beta_{k_0}) \in B_1$, then the next pair $(\alpha_{k_0+1},\beta_{k_0+1})$ lies in $R_{\mathcal{L}}$. If $(\alpha_{k_0},\beta_{k_0}) \in B_2 \cap R_{\mathcal{U}}$, then $(\alpha_{k_0+1},\beta_{k_0+1}) \in B_1 \subset R_{\mathcal{U}}$ and $(\alpha_{k_0+2},\beta_{k_0+2}) \in R_{\mathcal{L}}$. By symmetry considerations, it follows that the system stays inside R for all $k \geq k_0$. ■

So far, we have studied the precise evolution of the sequence $\{(\alpha_k,\beta_k)\}$ in the (α,β) plane. In Section IV, we will consider the step-wise reduction in the total error probability and deduce upper and lower bounds for it.

IV. Error Probability Bounds

In this section, we will first derive bounds for the total error probability in the case of equally likely hypotheses, where the fusion rule is the likelihood-ratio test with unit threshold. Then, we will deduce bounds for the total error probability in the case where the prior probabilities are unequal but the fusion rule remains the same.

The total error probability for a node with (α_k,β_k) is $(\alpha_k + \beta_k)/2$ in the case of equal prior probabilities. Let $L_k = \alpha_k + \beta_k$, namely, twice the total error probability. Analysis of the total error probability results from consideration of the sequence $\{L_k\}$. In fact, we will derive bounds on $\log L_k^{-1}$, whose growth rate is related to the rate of convergence of L_k to 0. We divide our analysis into two parts.

I We will study the shrinkage of the total error probability as the system propagates from B_m to B_1;

II We will study the shrinkage of the total error probability after the system enters B_1.

A. Case I: Error Probability Analysis as the System Propagates from B_m to B_1

Suppose that the initial state (α_0,β_0) lies in B_m, where m is a positive integer and $m \neq 1$. From the previous analysis, $(\alpha_{m-1},\beta_{m-1}) \in B_1$. In this section, we study the rate of reduction of the total error probability as the system propagates from B_m to B_1.

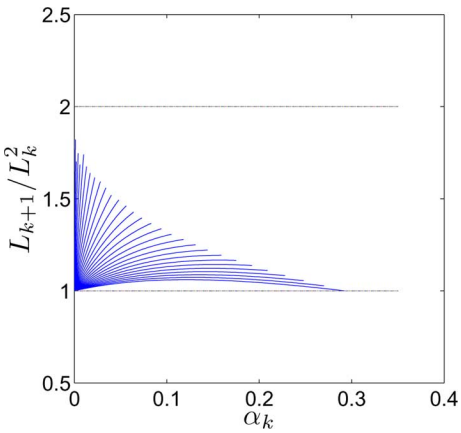

Fig. 5. Ratio L_{k+1}/L_k^2 in $\bigcup_{m=2}^{\infty} B_m$. Each line depicts the ratio versus α_k for a fixed β_k.

Proposition 2: Suppose that $(\alpha_k, \beta_k) \in B_m$, where m is a positive integer and $m \neq 1$. Then,

$$1 \leq \frac{L_{k+1}}{L_k^2} \leq 2.$$

The proof is given in Appendix A. Fig. 5 shows a plot of values of L_{k+1}/L_k^2 in $\bigcup_{m=2}^{\infty} B_m$. With the recursive relation given in Proposition 2, we can derive the following bounds for $\log L_k^{-1}$.

Proposition 3: Suppose that $(\alpha_0, \beta_0) \in B_m$, where m is a positive integer and $m \neq 1$. Then, for $k = 1, 2, \ldots, m-1$,

$$2^k \left(\log L_0^{-1} - 1\right) \leq \log L_k^{-1} \leq 2^k \log L_0^{-1}.$$

The proof is given in Appendix B. Suppose that the balanced binary relay tree has N leaf nodes. Then, the height of the fusion center is $\log N$. For convenience, let $P_N = L_{\log N}$ be (twice) the total error probability at the fusion center. Substituting $k = \log N$ into Proposition 3, we get the following result.

Corollary 1: Suppose that $(\alpha_0, \beta_0) \in B_m$, where m is a positive integer and $m \neq 1$. If $\log N < m$, then

$$N \left(\log L_0^{-1} - 1\right) \leq \log P_N^{-1} \leq N \log L_0^{-1}.$$

Notice that the lower bound of $\log P_N^{-1}$ is useful only if $L_0 < 1/2$. Next we derive a lower bound for $\log P_N^{-1}$ which is useful for all $L_0 \in (0, 1)$.

Proposition 4: Suppose that $(\alpha_k, \beta_k) \in B_m$, where m is a positive integer and $m \neq 1$. Then,

$$\frac{L_{k+1}}{L_k^{\sqrt{2}}} \leq 1.$$

The proof is given in Appendix C. Fig. 6 shows a plot of values of $L_{k+1}/L_k^{\sqrt{2}}$ in $\bigcup_{m=2}^{\infty} B_m$. With the inequality given in Proposition 4, we can derive a new lower bound for $\log P_N^{-1}$, which is useful for all $L_0 \in (0, 1)$.

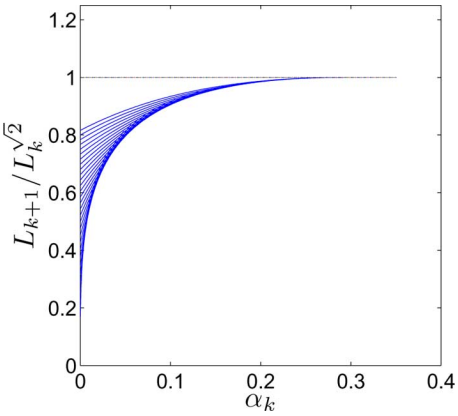

Fig. 6. Ratio $L_{k+2}/L_k^{\sqrt{2}}$ in $\bigcup_{m=2}^{\infty} B_m$. Each line depicts the ratio versus α_k for a fixed β_k.

Proposition 5: Suppose that $(\alpha_0, \beta_0) \in B_m$, where m is a positive integer and $m \neq 1$. If $\log N < m$, then

$$\log P_N^{-1} \geq \sqrt{N} \log L_0^{-1}.$$

The proof is given in Appendix D.

B. Case II: Error Probability Analysis When the System Stays inside R

We have derived error probability bounds up until the point where the trajectory of the system enters B_1. In this section, we consider the total error probability reduction from that point on. First, we will establish error probability bounds for even-height trees. Then, we will deduce error probability bounds for odd-height trees.

1) Error Probability Bounds for Even-Height Trees: If $(\alpha_0, \beta_0) \in B_m$ for some $m \neq 1$, then $(\alpha_{m-1}, \beta_{m-1}) \in B_1$. The system afterward stays inside the invariant region R (but not necessarily inside B_1). Hence, the decay rate of the total error probability in the invariant region R determines the asymptotic decay rate. Without loss of generality, we assume that (α_0, β_0) lies in the invariant region R. In contrast to Proposition 2, which bounds the ratio L_{k+1}/L_k^2, we will bound the ratio L_{k+2}/L_k^2 associated with taking two steps.

Proposition 6: Suppose that $(\alpha_k, \beta_k) \in R$. Then,

$$1 \leq \frac{L_{k+2}}{L_k^2} \leq 2.$$

The proof is given in Appendix E. Fig. 7(a) and (b) show plots of values of L_{k+2}/L_k^2 in B_1 and $B_2 \cap R_{\mathcal{U}}$, respectively.

Proposition 6 gives bounds on the relationship between L_k and L_{k+2} in the invariant region R. Hence, in the special case of trees with even height, that is, when $\log N$ is an even integer, it is easy to bound P_N in terms of L_0. In fact, we will bound $\log P_N^{-1}$ which in turn provides bounds for P_N.

Theorem 1: Suppose that $(\alpha_0, \beta_0) \in R$ and $\log N$ is even. Then,

$$\sqrt{N} \left(\log L_0^{-1} - 1\right) \leq \log P_N^{-1} \leq \sqrt{N} \log L_0^{-1}.$$

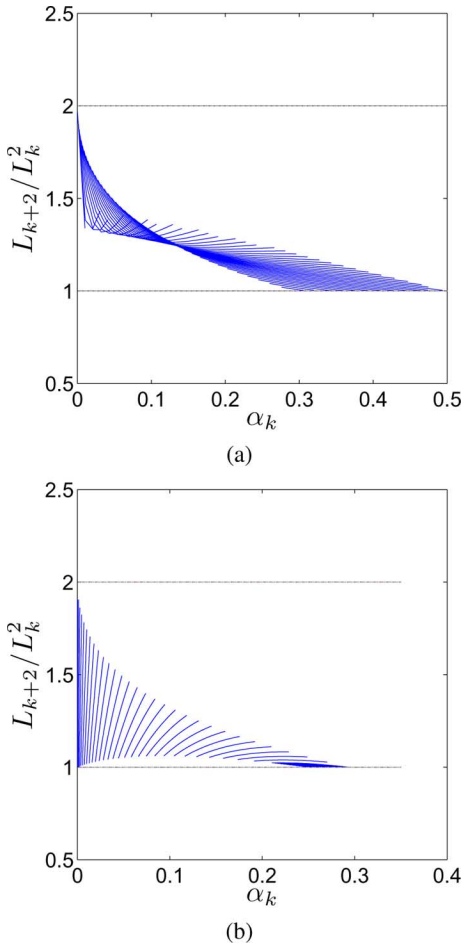

Fig. 7. (a) Ratio L_{k+2}/L_k^2 in B_1. (b) Ratio L_{k+2}/L_k^2 in $B_2 \cap R_{\mathcal{U}}$. Each line depicts the ratio versus α_k for a fixed β_k.

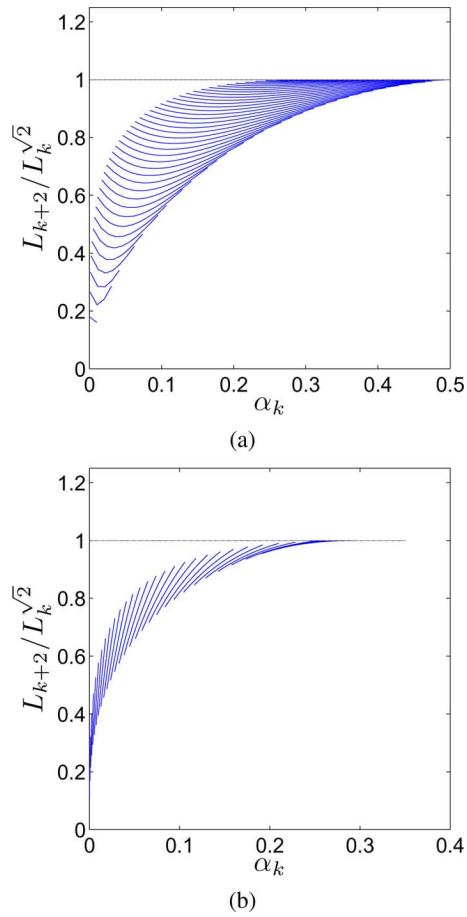

Fig. 8. (a) Ratio $L_{k+2}/L_k^{\sqrt{2}}$ in B_1. (b) Ratio $L_{k+2}/L_k^{\sqrt{2}}$ in $B_2 \cap R_{\mathcal{U}}$. Each line depicts the ratio versus α_k for a fixed β_k.

Proof: If $(\alpha_0, \beta_0) \in R$, then we have $(\alpha_k, \beta_k) \in R$ for $k = 0, 1, \ldots, \log N - 2$. From Proposition 6, we have

$$L_{k+2} = a_k L_k^2$$

for $k = 0, 2, \ldots, \log N - 2$ and some $a_k \in [1, 2]$. Therefore, for $k = 2, 4, \ldots, \log N$, we have

$$L_k = a_{(k-2)/2} \cdot a_{(k-4)/2}^2 \cdots a_0^{2^{(k-2)/2}} L_0^{2^{k/2}}$$

where $a_i \in [1, 2]$ for each i. Substituting $k = \log N$, we have

$$\begin{aligned} P_N &= a_{(k-2)/2} \cdot a_{(k-4)/2}^2 \cdots a_0^{2^{(k-2)/2}} L_0^{2^{\log \sqrt{N}}} \\ &= a_{(k-2)/2} \cdot a_{(k-4)/2}^2 \cdots a_0^{\sqrt{N}/2} L_0^{\sqrt{N}}. \end{aligned}$$

Hence

$$\begin{aligned} \log P_N^{-1} = &- \log a_{(k-2)/2} - 2 \log a_{(k-4)/2} - \cdots \\ &- \frac{\sqrt{N}}{2} \log a_0 + \sqrt{N} \log L_0^{-1}. \end{aligned}$$

Notice that $\log L_0^{-1} > 0$ and $0 \le \log a_i \le 1$ for each i. Thus,

$$\log P_N^{-1} \le \sqrt{N} \log L_0^{-1}.$$

Finally,

$$\begin{aligned} \log P_N^{-1} &\ge -1 - 2 - \cdots - \frac{\sqrt{N}}{2} + \sqrt{N} \log L_0^{-1} \\ &\ge -\sqrt{N} + \sqrt{N} \log L_0^{-1} = \sqrt{N} \left(\log L_0^{-1} - 1 \right). \end{aligned}$$

■

Notice that the lower bound for $\log P_N^{-1}$ in Theorem 1 is useful only if $L_0 < 1/2$. We further provide a lower bound for $\log P_N^{-1}$ which is useful for all $L_0 \in (0, 1)$.

Proposition 7: Suppose that $(\alpha_k, \beta_k) \in R$. Then,

$$\frac{L_{k+2}}{L_k^{\sqrt{2}}} \le 1.$$

The proof is given in Appendix F. Fig. 8(a) and (b) show plots of the ratio inside B_1 and $B_2 \cap R_{\mathcal{U}}$, respectively. Next, we derive a new lower bound for $\log P_N^{-1}$.

Proposition 8: Suppose that $(\alpha_0, \beta_0) \in R$ and $\log N$ is even. Then,

$$\log P_N^{-1} \ge \sqrt[4]{N} \log L_0^{-1}.$$

The proof is given in Appendix G.

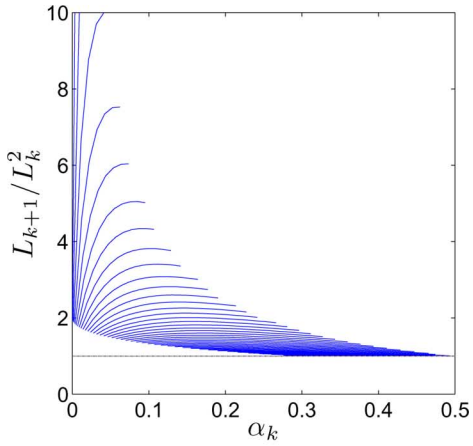

(a)

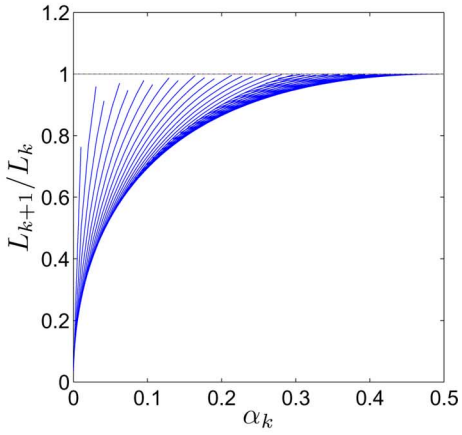

(b)

Fig. 9. (a) Ratio L_{k+1}/L_k^2 in $\mathcal{U}$. (b) Ratio L_{k+1}/L_k in $\mathcal{U}$. Each line depicts the ratio versus α_k for a fixed β_k.

2) Error Probability Bounds for Odd-Height Trees: Next we explore the case of trees with odd height; i.e., $\log N$ is an odd integer. Assume that (α_0, β_0) lies in the invariant region R. First, we will establish general bounds for odd-height trees. Then we deduce bounds for the case where there exists $(\alpha_m, \beta_m) \in B_2 \cap R_{\mathcal{U}}$ for some $m \in \{0, 1, \ldots, \log N - 2\}$.

For odd-height trees, we need to know how much the total error probability is reduced by moving up one level in the tree.

Proposition 9: Suppose that $(\alpha_k, \beta_k) \in \mathcal{U}$. Then,

$$1 \leq \frac{L_{k+1}}{L_k^2}$$

and

$$\frac{L_{k+1}}{L_k} \leq 1.$$

The proof is given in Appendix H. Fig. 9(a) and (b) show plots of values of L_{k+1}/L_k^2 and L_{k+1}/L_k in $\mathcal{U}$.

Using Propositions 6 and 9, we are about to calculate error probability bounds for odd-height trees as follows.

Theorem 2: Suppose that $(\alpha_0, \beta_0) \in R$ and $\log N$ is odd. Then,

$$\sqrt{\frac{N}{2}}\left(\log L_0^{-1} - 1\right) \leq \log P_N^{-1} \leq \sqrt{2N} \log L_0^{-1}.$$

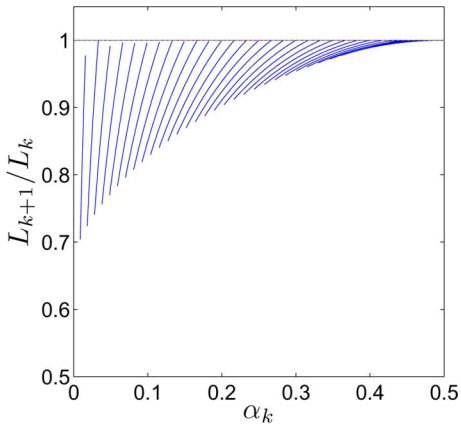

Fig. 10. Ratio L_{k+1}/L_k in the region $f(B_2 \cup R_{\mathcal{U}})$. Each line depicts the ratio versus α for a fixed β.

The proof is given in Appendix I. Next we consider the special case where there exists $m \in \{0, 1, \ldots, \log N - 2\}$ such that $(\alpha_m, \beta_m) \in B_2 \cap R_{\mathcal{U}}$.

Proposition 10: Suppose that $(\alpha_k, \beta_k) \in B_1$ and $(\alpha_{k-1}, \beta_{k-1}) \in B_2 \cap R_{\mathcal{U}}$. Then,

$$\frac{1}{2} \leq \frac{L_{k+1}}{L_k} \leq 1.$$

The proof is given in Appendix J. Fig. 10 shows a plot of values of L_{k+1}/L_k in this case.

We have proved in Proposition 6 that if (α_k, β_k) is in $B_2 \cap R_{\mathcal{U}}$, then the ratio $L_{k+2}/L_k^2 \in [1, 2]$. However, if we analyze each level of fusion, it can be seen that the total error probability decreases exponentially fast from $B_2 \cap R_{\mathcal{U}}$ to B_1 (see Proposition 2). Proposition 10 tells us that the fusion from B_1 to $R_{\mathcal{L}}$ is a bad step, which does not contribute significantly in decreasing the total error probability.

We can now provide bounds for the total error probability at the fusion center.

Theorem 3: Suppose that $(\alpha_0, \beta_0) \in R$, $\log N$ is an odd integer, and there exists $m \in \{0, 1, \ldots, \log N - 2\}$ such that $(\alpha_m, \beta_m) \in B_2 \cap R_{\mathcal{U}}$.

If m is even, then

$$\sqrt{2N}\left(\log L_0^{-1} - 1\right) \leq \log P_N^{-1} \leq \sqrt{2N} \log L_0^{-1}.$$

If m is odd, then

$$\sqrt{\frac{N}{2}}\left(\log L_0^{-1} - 1\right) \leq \log P_N^{-1} \leq \sqrt{\frac{N}{2}} \log L_0^{-1} + \sqrt{\frac{N}{2^{m+2}}}.$$

The proof is given in Appendix K. Finally, by combining all of the aforementioned analysis for step-wise reduction of the total error probability, we can write general bounds when the initial error probability pair (α_0, β_0) lies inside B_m, where $m \neq 1$.

Theorem 4: Suppose that $(\alpha_0, \beta_0) \in B_m$, where m is an integer and $m \neq 1$.

If $\log N < m$, then (*Corollary 1*)

$$N\left(\log L_0^{-1} - 1\right) \leq \log P_N^{-1} \leq N \log L_0^{-1}.$$

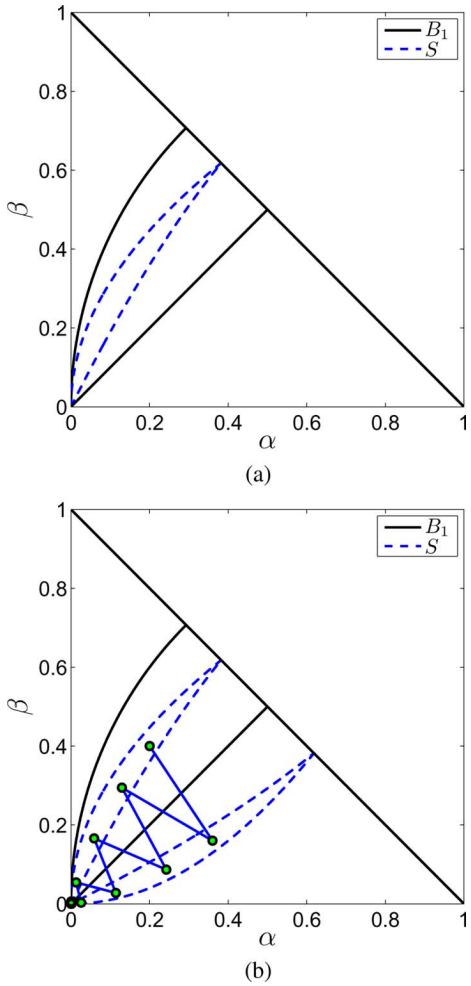

Fig. 11. (a) Invariant region S (between dashed lines) lies inside B_1 (between solid lines). (b) Trajectory of the system which stays inside S.

If $\log N \geq m$, and $\log N - m$ is odd, then

$$\sqrt{2^{m-1}N}\left(\log L_0^{-1} - 1\right) \leq \log P_N^{-1} \leq \sqrt{2^{m-1}N}\log L_0^{-1}.$$

If $\log N \geq m$, and $\log N - m$ is even, then

$$\sqrt{2^{m-2}N}\left(\log L_0^{-1} - 1\right) \leq \log P_N^{-1} \leq \sqrt{2^{m}N}\log L_0^{-1}.$$

The proof uses similar arguments as that of Theorem 2 and it is provided in Appendix L.

Remark: Notice again that the lower bounds for $\log P_N^{-1}$ above are useful only if $L_0 < 1/2$. However, similar to Proposition 8, we can derive a lower bound for $\log P_N^{-1}$, which is useful for all $L_0 \in (0,1)$. It turns out that this lower bound differs from that in Proposition 8 by a constant term. Therefore, it is omitted.

C. Invariant Region in B_1

Consider the region $\{(\alpha,\beta) \in \mathcal{U} | \beta \leq \sqrt{\alpha} \text{ and } \beta \geq 1-(1-\alpha)^2\}$, which is a subset of B_1 [see Fig. 11(a)]. Denote the union of this region and its reflection with respect to $\beta = \alpha$ by S. It turns out that S is also invariant.

Proposition 11: If $(\alpha_{k_0}, \beta_{k_0}) \in S$, then $(\alpha_k, \beta_k) \in S$ for all $k \geq k_0$.

The proof is given in Appendix M. Fig. 11(b) shows a single trajectory of the dynamic system which stays inside S.

We have given bounds for P_N, which is (twice) the total error probability. It turns out that for the case where $(\alpha_0, \beta_0) \in S$, we can bound the Type I and Type II errors individually.

Proposition 12: If $(\alpha_k, \beta_k) \in S$, then

$$1 \leq \frac{\alpha_{k+2}}{\alpha_k^2} \leq 4$$

and

$$1 \leq \frac{\beta_{k+2}}{\beta_k^2} \leq 4.$$

Remark: It is easy to see that as long as the system stays inside B_1, then in a similar vein, these ratios α_{k+2}/α_k^2 and β_{k+2}/β_k^2 are lower bounded by 1 and upper bounded by a constant. But recall that B_1 is not an invariant region. Thus, it is more interesting to consider S.

Proofs are omitted because they are along similar lines to those in the other proofs. As before, these inequalities give rise to bounds on sequences $\{\alpha_k\}$ and $\{\beta_k\}$. For example, for $\{\alpha_k\}$, we have the following.

Corollary 2: If $(\alpha_0, \beta_0) \in S$ and k is even, then

$$2^{k/2}\left(\log \alpha_0^{-1} - 2\right) \leq \log \alpha_k^{-1} \leq 2^{k/2}\log \alpha_0^{-1}.$$

D. Unequal Likely Hypotheses

In this section, we consider the situation of unequally likely hypotheses; that is, $P(H_0) \neq P(H_1)$. Suppose that the fusion rule is as before: the likelihood ratio test with unit threshold. The resulting total error probability for the nodes at level k is equal to $\hat{L}_k = P(H_0)\alpha_k + P(H_1)\beta_k$, and the total error probability at the fusion center is $\hat{P}_N = \hat{L}_{\log N}$. We are interested in bounds for $\hat{P}_N$.

Because the fusion rule is the same as before, the previous bounds for $\log L_k^{-1}$ hold. From these bounds, we now derive bounds for $\hat{P}_N$. Without loss of generality, we assume that $P(H_0) \leq P(H_1)$. We obtain the following:

$$P(H_0)L_k \leq P(H_0)\alpha_k + P(H_1)\beta_k \leq P(H_1)L_k.$$

From these inequalities, we can derive upper and lower bounds for $\log \hat{P}_N^{-1}$. For example, in the case where $(\alpha_0, \beta_0) \in R$ and $\log N$ is even (even-height tree), from Theorem 1, we have

$$\sqrt{N}(\log L_0^{-1} - 1) \leq \log P_N^{-1} \leq \sqrt{N}\log L_0^{-1},$$

from which we obtain

$$\sqrt{N}(\log L_0^{-1} - 1) + \log P(H_1)^{-1} \leq \log \hat{P}_N^{-1} \leq \sqrt{N}\log L_0^{-1} + \log P(H_0)^{-1}.$$

We have derived error probability bounds for balanced binary relay trees under several scenarios. In Section V, we will use these bounds to study the asymptotic rate of convergence.

V. Asymptotic Rates

The asymptotic decay rate of the total error probability with respect to N while the performance of the sensors is constant is the first problem to be tackled. Then we allow the sensors to be asymptotically crummy, in the sense that $\alpha_0+\beta_0 \to 1$. We prove that the total error probability still converges to 0 under certain conditions. Finally, we will compare the detection performance by applying different strategies in balanced binary relay trees.

In this section, we use the following notation: for positive functions f and g defined on the positive integers, if there exist positive constants c_1 and c_2 such that $c_1 g(N) \le f(N) \le c_2 g(N)$ for all sufficiently large N, then we write $f(N) = \Theta(g(N))$. For $N \to \infty$, the notation $f(N) \sim g(N)$ means that $f(N)/g(N) \to 1$, $f(N) = \omega(g(N))$ that $f(N)/g(N) \to \infty$, and $f(N) = o(g(N))$ that $f(N)/g(N) \to 0$.

A. Asymptotic Decay Rate

Notice that as N becomes large, the sequence $\{(\alpha_k, \beta_k)\}$ will eventually move into the invariant region R at some level and stays inside from that point. Therefore, it suffices to consider the decay rate in the invariant region R. Because error probability bounds for trees with odd height differ from those of the even-height tree by a constant term, without loss of generality, we will only consider trees with even height.

Proposition 13: If $L_0 = \alpha_0 + \beta_0$ is fixed, then

$$\log P_N^{-1} = \Theta(\sqrt{N}).$$

Proof: If $L_0 = \alpha_0 + \beta_0$ is fixed, then by Proposition 8 we immediately see that $P_N \to 0$ as $N \to \infty$ ($\log P_N^{-1} \to \infty$) and there exists a finite k such that $L_k < 1/2$. To analyze the asymptotic rate, we may assume that $L_0 < 1/2$. In this case, the bounds in Theorem 1 show that

$$\log P_N^{-1} = \Theta(\sqrt{N}).$$

■

This implies that the convergence of the total error probability is subexponential; more precisely, the exponent is essentially $\sqrt{N}$.

In the special case where $(\alpha_0, \beta_0) \in S$, the Type I and Type II error probabilities decay to 0 with exponent $\sqrt{N}$ individually. Moreover, it is easy to show that the exponent is still $\sqrt{N}$ even if the prior probabilities are unequal.

Given $L_0 \in (0,1)$ and $\varepsilon \in (0,1)$, suppose that we wish to determine how many sensors we need to have so that $P_N \le \varepsilon$. If $L_0 < 1/2$, then the solution is simply to find N (e.g., the smallest) satisfying the inequality

$$\sqrt{N}\left(\log L_0^{-1} - 1\right) \ge -\log \varepsilon.$$

In consequence, we have

$$N \ge \left((\log L_0^{-1} - 1)\log \varepsilon\right)^2.$$

The smallest N grows like $\Theta((\log \varepsilon)^2)$ (cf., [32], in which the smallest N has a larger growth rate). If $L_0 \ge 1/2$, then by Proposition 8 we can deduce how many levels k are required so that $L_k < 1/2$:

$$\sqrt[4]{N} \log L_0^{-1} > -\log \frac{1}{2} = 1.$$

Therefore, N has to satisfy

$$N > (\log L_0^{-1})^{-4}$$

which implies that

$$k > 4 \log(\log {L_0}^{-1})^{-1}.$$

Combining with the aforementioned analysis for the case where $L_0 < 1/2$, we can then determine the number of sensors required so that $P_N \le \varepsilon$.

B. Crummy Sensors

In this section, we allow the total error probability of each sensor, denoted by $L_0^{(N)}$, to depend on N but still to be constant across sensors.

If $L_0^{(N)}$ is bounded by some constant $L \in (0,1)$ for all N, then clearly $P_N \to 0$. It is more interesting to consider $L_0^{(N)} \to 1$, which means that sensors are asymptotically crummy.

Proposition 14: Suppose that $L_0^{(N)} = 1 - \eta_N$ with $\eta_N \to 0$.

1) If $\eta_N \ge c_1/\sqrt[4]{N}$, then $P_N \le e^{-c_1}$.
2) If $\eta_N = \omega(1/\sqrt[4]{N})$, then $P_N \to 0$.
3) If $\eta_N \le c_2/\sqrt{N}$, then $P_N \ge e^{-c_2}$.
4) If $\eta_N = o(1/\sqrt{N})$, then $P_N \to 1$.

Proof: First, we consider part (1). We have

$$\sqrt[4]{N} \log(L_0^{(N)})^{-1} = -\sqrt[4]{N} \log(1 - \eta_N).$$

But as $x \to 0$, $-\log(1-x) \sim x/\ln(2)$, from which we obtain

$$\sqrt[4]{N} \log(L_0^{(N)})^{-1} \sim \eta_N \sqrt[4]{N}/\ln(2).$$

From Proposition 8, it is easy to see that if we have $\eta_N \ge c_1/\sqrt[4]{N}$, then for sufficiently large N we obtain

$$\log P_N^{-1} \ge \sqrt[4]{N} \log(L_0^{(N)})^{-1} \ge c_1/\ln(2)$$

that is,

$$P_N \le 2^{-c_1/\ln(2)} = e^{-c_1}.$$

Moreover, if $\eta_N \sqrt[4]{N} \to \infty$, that is, $\eta_N = \omega(1/\sqrt[4]{N})$, then $P_N \to 0$. This finishes the proof for part (2).

Next we consider parts (3) and (4). We have

$$\sqrt{N} \log(L_0^{(N)})^{-1} = -\sqrt{N} \log(1 - \eta_N)$$

from which we obtain

$$\sqrt{N} \log(L_0^{(N)})^{-1} \sim \eta_N \sqrt{N}/\ln(2).$$

From Theorem 1, it is easy to see that if we have $\eta_N \leq c_2/\sqrt{N}$, then for sufficiently large N we obtain

$$\log P_N^{-1} \leq \sqrt{N} \log(L_0^{(N)})^{-1} \leq c_2/\ln(2)$$

that is,

$$P_N \geq 2^{-c_2/\ln(2)} = e^{-c_2}.$$

Moreover, if $\eta_N\sqrt{N} \to \infty$, that is, $\eta_N = o(1/\sqrt{N})$, then $P_N \to 1$. ■

Using part (3) of the aforementioned proposition, we derive a necessary condition for $P_N \to 0$.

Corollary 3: Suppose that $L_0^{(N)} = 1 - \eta_N$ with $\eta_N \to 0$. Then, $P_N \to 0$ implies that $\eta_N = \omega(1/\sqrt{N})$.

C. Comparison of Simulation Results

We end this section by comparing the quantitative behavior of the unit-threshold likelihood-ratio rule with that of other fusion rules of interest. First, we define two particular fusion rules that can be applied at an individual node.

1) OR rule: the parent node decides 0 if and only if both the child nodes send 0.
2) AND rule: the parent node decides 1 if and only if both the child nodes send 1.

Notice that the unit-threshold likelihood-ratio rule reduces to either the AND rule or the OR rule, depending on the values of the Type I and Type II error probabilities at the particular level of the tree. For our quantitative comparison, we consider three system-wide fusion strategies that we will compare with the case that uses the unit-threshold likelihood-ratio rule at every node.

1) OR strategy: every fusion uses the OR rule.
2) AND strategy: every fusion uses the AND rule.
3) RAND strategy: at each level of the tree, we randomly pick either the AND rule or the OR rule with equal probability, and independently over levels, and apply that rule to all the nodes at that level.

In Fig. 12, we show plots of the total error probability as a function of N for the tree that uses the unit-threshold likelihood-ratio rule at every node (the one analyzed in this paper). We also plot the total error probabilities for the AND and OR strategies, as well as the average total error probability over 100 independent trials of the RAND strategy. For comparison purposes, we also plot the error probability curve of the centralized parallel fusion strategy.

We can see from Fig. 12 that the total error probability for the centralized parallel strategy decays to 0 faster than that of the binary relay tree that uses the unit-threshold likelihood-ratio rule at every node. This is not surprising because the former is known to be exponential, as discussed earlier, while the latter is subexponential with exponent $\sqrt{N}$, as shown in this paper. The AND and OR strategies both result in total error probabilities converging monotonically to $1/2$, while the RAND strategy results in an average total error probability that does not decrease much with N.

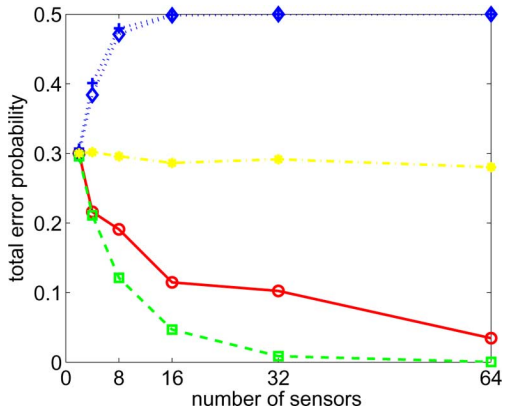

Fig. 12. Total error probability plots. Dashed line: centralized parallel fusion strategy. Solid line: unit-threshold likelihood-ratio rule for the balanced binary relay tree. Dotted line with "◇" marker: OR strategy. Dotted line with "+" marker: AND strategy. Dash-dotted line: RAND strategy.

VI. Concluding Remarks

We have studied the detection performance of balanced binary relay trees. We precisely describe the evolution of error probabilities in the (α, β) plane as we move up the tree. This allows us to deduce error probability bounds at the fusion center as functions of N under several different scenarios. These bounds show that the total error probability converges to 0 subexponentially, with an exponent that is essentially $\sqrt{N}$. In addition, we allow all sensors to be asymptotically crummy, in which case we deduce the necessary and sufficient conditions for the total error probability to converge to 0. All our results apply not only to the fusion center, but also to any other node in the tree network. In other words, we can similarly analyze a subtree inside the original tree network.

Our approach also generalizes to arbitrary balanced relay trees where each node except the leaf node has $M \geq 2$ child nodes (M-ary tree). Moreover, we can also treat the case where we allow more general (nonbinary) message alphabets. Specifically, we can show that the error probability analysis in these cases is essentially equivalent to that of corresponding M-ary trees with binary alphabets. The detailed calculations are beyond the scope of this paper. To illustrate the connection between more general message alphabets and M-ary trees, consider the simplest extension from binary to ternary message alphabets in a balanced binary (2-ary) relay tree. Suppose that each sensor makes a binary decision based on the measurement and then sends the binary message upward to its parent node at level 1. Then, for each node at level 1, we can combine the two binary messages from its children (sensors) into a ternary message without losing any information. As a result, the performance in this scenario is the same as that of a tree in which each node at level 2 connects to four sensors directly. Suppose that we repeat this process recursively throughout the tree. Then, to study the performance of balanced binary relay trees with ternary message alphabets, equivalently we can analyze 4-ary trees with binary alphabets. In this case, it turns out that if we simply apply *majority dominance* (with random tie-breaking) as the fusion rule, then the total error probability decays to 0 with exponent $\sqrt{N}$.

Needless to say, our conclusions are subject to our particular architecture and assumptions. Several questions follow. Considering balanced binary relay trees with sensor and/or communication link failures, how would the error probabilities behave? More generally, what can we say about unbalanced relay trees? In addition, how would the performance change if all the relay nodes make their own measurements? These and other related questions are being investigated.

Appendix A
Proof of Proposition 2

If $(\alpha_k, \beta_k) \in B_m$, where m is a positive integer and $m \neq 1$, then

$$\frac{L_{k+1}}{L_k^2} = \frac{1-(1-\alpha_k)^2+\beta_k^2}{(\alpha_k+\beta_k)^2}.$$

The following calculation establishes the lower bound of the ratio L_{k+1}/L_k^2:

$$\begin{aligned} L_{k+1} - L_k^2 &= 1-(1-\alpha_k)^2+\beta_k^2-(\alpha_k+\beta_k)^2 \\ &= -2\alpha_k^2 - 2\alpha_k\beta_k + 2\alpha_k \\ &= 2\alpha_k(1-(\alpha_k+\beta_k)) \geq 0 \end{aligned}$$

which holds in B_m.

To show the upper bound of the ratio L_{k+1}/L_k^2, it suffices to prove that

$$\begin{aligned} L_{k+1} - 2L_k^2 &= 1-(1-\alpha_k)^2+\beta_k^2-2(\alpha_k+\beta_k)^2 \\ &= -3\alpha_k^2 - 4\alpha_k\beta_k + 2\alpha_k - \beta_k^2 \leq 0. \end{aligned}$$

The partial derivative with respect to β_k is

$$\frac{\partial(L_{k+1}-2L_k^2)}{\partial\beta_k} = -2\beta_k - 4\alpha_k \leq 0$$

which is nonpositive, and so it suffices to consider values on the upper boundary of B_1

$$\begin{aligned} L_{k+1} - 2L_k^2 &= 1-(1-\alpha_k)^2+\beta_k^2-2(\alpha_k+\beta_k)^2 \\ &= 2\beta_k^2 - 2(\alpha_k+\beta_k)^2 \leq 0. \end{aligned}$$

In consequence, the claimed upper bound on the ratio L_{k+1}/L_k^2 holds.

Appendix B
Proof of Proposition 3

From Proposition 2 we have, for $k = 0, 1, \ldots, m-2$,

$$L_{k+1} = a_k L_k^2$$

for some $a_k \in [1, 2]$. Then, for $k = 1, 2, \ldots, m-1$

$$L_k = a_{k-1} \cdot a_{k-2}^2 \ldots a_0^{2^{k-1}} L_0^{2^k}$$

where $a_i \in [1, 2]$ for each i. Hence

$$\begin{aligned} \log L_k^{-1} = &-\log a_{k-1} - 2\log a_{k-2} - \cdots \\ &- 2^{k-1}\log a_0 - \log L_0^{2^k}. \end{aligned}$$

Since $\log L_0^{-1} > 0$ and $0 \leq \log a_i \leq 1$ for each i, we have

$$\log L_k^{-1} \leq 2^k \log L_0^{-1}.$$

Finally,

$$\begin{aligned} \log L_k^{-1} &\geq -1-2-\cdots-2^{k-1}+2^k\log L_0^{-1} \\ &\geq -2^k + 2^k \log L_0^{-1} = 2^k\left(\log L_0^{-1} - 1\right). \end{aligned}$$

Appendix C
Proof of Proposition 4

If $(\alpha_k, \beta_k) \in B_m$, where m is a positive integer and $m \neq 1$, then

$$\frac{L_{k+1}}{L_k^{\sqrt{2}}} = \frac{1-(1-\alpha_k)^2+\beta_k^2}{(\alpha_k+\beta_k)^{\sqrt{2}}}.$$

To prove the upper bound of the ratio, it suffices to show that

$$\psi(\alpha_k, \beta_k) = 1-(1-\alpha_k)^2+\beta_k^2-(\alpha_k+\beta_k)^{\sqrt{2}} \leq 0.$$

The second-order partial derivative of ψ with respect to α_k is nonpositive:

$$\frac{\partial^2\psi}{\partial\alpha_k^2} = -2 - \sqrt{2}(\sqrt{2}-1)(\alpha_k+\beta_k)^{\sqrt{2}-2} \leq 0.$$

Therefore, the minimum of $\partial\psi/\partial\alpha_k$ is on the lines $\alpha_k+\beta_k = 1$ and $(1-\alpha_k)^2+\beta_k^2 = 1$. It is easy to show that $\partial\psi/\partial\alpha_k \geq 0$. In consequence, the maximum of ψ is on the lines $\alpha_k+\beta_k = 1$ and $(1-\alpha_k)^2+\beta_k^2 = 1$. If $\alpha_k+\beta_k = 1$, then it is easy to see that $\psi = 0$. If $(1-\alpha_k)^2+\beta_k^2 = 1$, then $\psi = 2\beta_k^2 - (\alpha_k+\beta_k)^{\sqrt{2}}$. It is easy to show that the maximum value of ψ lies at the intersection of $\alpha_k+\beta_k = 1$ and $(1-\alpha_k)^2+\beta_k^2 = 1$, where $\psi = 0$. Hence, the ratio $L_{k+1}/L_k^{\sqrt{2}}$ is upper bounded by 1.

Appendix D
Proof of Proposition 5

From Proposition 4 we have, for $k = 0, 1, \ldots, m-2$,

$$L_{k+1} = a_k L_k^{\sqrt{2}}$$

for some $a_k \in (0, 1]$. Then, for $k = 1, 2, \ldots, m-1$,

$$L_k = a_{k-1} \cdot a_{k-2}^{\sqrt{2}} \ldots a_0^{\sqrt{2}^{k-1}} L_0^{\sqrt{2}^k}$$

where $a_i \in (0, 1]$ for each i. Hence,

$$\begin{aligned} \log L_k^{-1} = &-\log a_{k-1} - \sqrt{2}\log a_{k-2} - \cdots \\ &- \sqrt{2}^{k-1}\log a_0 - \log L_0^{\sqrt{2}^k}. \end{aligned}$$

Since $\log L_0^{-1} > 0$ and $\log a_i \le 0$ for each i, we have

$$\log L_k^{-1} \ge \sqrt{2}^k \log L_0^{-1}.$$

Therefore, we have

$$\log P_N^{-1} \ge \sqrt{N} \log L_0^{-1}.$$

Appendix E
Proof of Proposition 6

Because of symmetry, we only have to prove the case where (α_k, β_k) lies in $R_{\mathcal{U}}$. We consider two cases: $(\alpha_k, \beta_k) \in B_1$ and $(\alpha_k, \beta_k) \in B_2 \cap R_{\mathcal{U}}$.

In the first case

$$\frac{L_{k+2}}{L_k^2} = \frac{(1-(1-\alpha_k)^2)^2 + 1 - (1-\beta_k^2)^2}{(\alpha_k+\beta_k)^2}.$$

To prove the lower bound of the ratio, it suffices to show that

$$\begin{aligned} L_{k+2} - L_k^2 &= (1-(1-\alpha_k)^2)^2 + 1 - (1-\beta_k^2)^2 - (\alpha_k+\beta_k)^2 \\ &= (1-\alpha_k-\beta_k)((\beta_k-\alpha_k)^3 + 2\alpha_k\beta_k(\beta_k-\alpha_k) \\ &\quad + (\beta_k-\alpha_k)^2 + 2\alpha_k^2) \ge 0. \end{aligned}$$

We have $1-\alpha_k-\beta_k > 0$ and $\beta_k \ge \alpha_k$ for all $(\alpha_k, \beta_k) \in B_1$, resulting in the aforementioned inequality.

To prove the upper bound of the ratio, it suffices to show that

$$L_{k+2} - 2L_k^2 = \alpha_k^4 - 4\alpha_k^3 + 2\alpha_k^2 - 4\alpha_k\beta_k - \beta_k^4 \le 0.$$

The partial derivative with respect to β_k is

$$\frac{\partial(L_{k+2} - 2L_k^2)}{\partial \beta_k} = -4\alpha_k - 4\beta_k^3 \le 0$$

which is nonpositive. Therefore, it suffices to consider its values on the curve $\beta_k = \alpha_k$, on which $L_{k+2} - 2L_k^2$ is clearly nonpositive.

Now we consider the second case, namely $(\alpha_k, \beta_k) \in B_2 \cap R_{\mathcal{U}}$, which gives

$$\frac{L_{k+2}}{L_k^2} = \frac{1-(1-\alpha_k)^4 + \beta_k^4}{(\alpha_k+\beta_k)^2}.$$

To prove the lower bound of the ratio, it suffices to show that

$$\begin{aligned} L_{k+2} - L_k^2 &= (1-(1-\alpha_k)^4) + \beta_k^4 - (\alpha_k+\beta_k)^2 \\ &= (1-\alpha_k-\beta_k)(\alpha_k^3 - \alpha_k^2\beta_k - 3\alpha_k^2 + \alpha_k\beta_k^2 \\ &\quad + 2\alpha_k\beta_k - \beta_k^3 - \beta_k^2 + 4\alpha_k) \ge 0. \end{aligned}$$

Therefore, it suffices to show that

$$\begin{aligned} \phi(\alpha_k, \beta_k) &= \alpha_k^3 - \alpha_k^2\beta_k - 3\alpha_k^2 + \alpha_k\beta_k^2 \\ &\quad + 2\alpha_k\beta_k - \beta_k^3 - \beta_k^2 + 4\alpha_k \ge 0. \end{aligned}$$

The partial derivative with respect to β_k is

$$\frac{\partial \phi}{\partial \beta_k} = -(\alpha_k-\beta_k)^2 - 2\beta_k^2 + 2(\alpha_k-\beta_k) \le 0.$$

Thus, it is enough to consider the values on the upper boundaries $\sqrt{1-\beta_k} + \sqrt{\alpha_k} = 1$ and $\alpha_k + \beta_k = 1$.

If $\alpha_k + \beta_k = 1$, then the inequality is trivial, and if $\sqrt{1-\beta_k} + \sqrt{\alpha_k} = 1$, then

$$L_{k+2} - L_k^2 = 2\alpha_k^2(1-2\sqrt{\alpha_k})(2\alpha_k - 6\sqrt{\alpha_k} + 5)$$

and the inequality holds because $\alpha_k \le \frac{1}{4}$ in region $B_2 \cap R_{\mathcal{U}}$.

The claimed upper bound for the ratio L_{k+2}/L_k^2 can be written as

$$\begin{aligned} L_{k+2} - 2L_k^2 &= (1-(1-\alpha_k)^4) + \beta_k^4 - 2(\alpha_k+\beta_k)^2 \\ &= -\alpha_k^4 + 4\alpha_k^3 - 8\alpha_k^2 + 4\alpha_k \\ &\quad - 4\alpha_k\beta_k + \beta_k^4 - 2\beta_k^2 \le 0. \end{aligned}$$

The partial derivative with respect to β_k is

$$\frac{\partial(L_{k+2} - 2L_k^2)}{\partial \beta_k} = -4\alpha_k + 4\beta_k^3 - 4\beta_k \le 0.$$

Again, it is sufficient to consider values on the upper boundary of B_1. Hence,

$$L_{k+2} - 2L_k^2 = 2\beta_k^2 - 2(\alpha_k+\beta_k)^2 \le 0.$$

Appendix F
Proof of Proposition 7

In the case where $(\alpha_k, \beta_k) \in B_2 \cap R_{\mathcal{U}}$, from Proposition 4, we have $L_{k+1} \le L_k^{\sqrt{2}}$. Moreover, it is easy to show that $L_{k+2} \le L_{k+1}$. Thus, we have $L_{k+2} \le L_k^{\sqrt{2}}$.

In the case where $(\alpha_k, \beta_k) \in B_1$, it suffices to prove that

$$\vartheta(\alpha_k, \beta_k) = (1-(1-\alpha_k)^2)^2 + 1 - (1-\beta_k^2)^2 - (\alpha_k+\beta_k)^{\sqrt{2}} \le 0.$$

We take second-order partial derivative of ϑ with respect to α_k along the lines $\alpha_k + \beta_k = c$ in this region. It is easy to show that the derivative is non-negative:

$$\frac{\partial^2 \vartheta}{\partial \alpha_k^2} = 12((1-\alpha_k)^2 - \beta_k^2) \ge 0.$$

Therefore, we conclude that the maximum of ϑ lies on the boundaries of this region. If $\alpha_k + \beta_k = 1$, then we have $\vartheta(\alpha_k, \beta_k) = 0$. If $(1-\alpha_k)^2 + \beta_k^2 = 1$, then we have $\alpha_{k+1} = \beta_{k+1}$. Moreover, if $\alpha_{k+1} = \beta_{k+1}$, then we can show that $L_{k+2} = L_{k+1}$. Hence, it suffices to show that $L_{k+1}/L_k^{\sqrt{2}} \le 1$ on the line $(1-\alpha_k)^2 + \beta_k^2 = 1$, which has been proved in Proposition 4. If $\beta_k = \alpha_k$, then $L_{k+1} = L_k$ and $(\alpha_{k+1}, \beta_{k+1})$ lies on the lower boundary of $R_{\mathcal{L}}$, on which we have $L_{k+2}/L_{k+1}^{\sqrt{2}} \le 1$. Thus, we have $L_{k+2}/L_k^{\sqrt{2}} \le 1$.

APPENDIX G
PROOF OF PROPOSITION 8

From Proposition 7 we have, for $k = 0, 2, \ldots, \log N - 2$,

$$L_{k+2} = a_k L_k^{\sqrt{2}}$$

for some $a_k \in (0, 1]$. Then, for $k = 2, 4, \ldots, \log N$, we have

$$L_k = a_{(k-2)/2} \cdot a_{(k-4)/2}^{\sqrt{2}} \ldots a_0^{\sqrt{2}^{(k-2)/2}} L_0^{\sqrt{2}^{k/2}}$$

where $a_i \in (0, 1]$ for each i. Therefore,

$$\begin{aligned}\log L_k^{-1} = &- \log a_{(k-2)/2} - \sqrt{2} \log a_{(k-4)/2} - \cdots \\ &- \sqrt{2}^{(k-2)/2} \log a_0 - \log L_0^{\sqrt{2}^{k/2}}.\end{aligned}$$

Since $\log L_0^{-1} > 0$ and $\log a_i \leq 0$ for each i, we have

$$\log L_k^{-1} \geq \sqrt{2}^{k/2} \log L_0^{-1}.$$

Therefore, we have

$$\log P_N^{-1} \geq \sqrt[4]{N} \log L_0^{-1}.$$

APPENDIX H
PROOF OF PROPOSITION 9

The first inequality is equivalent to

$$\begin{aligned}L_{k+1} - L_k^2 &= 1 - (1 - \alpha_k)^2 + \beta_k^2 - (\alpha_k + \beta_k)^2 \\ &= 2\alpha_k(1 - (\alpha_k + \beta_k)) \geq 0\end{aligned}$$

which holds for all $(\alpha_k, \beta_k) \in \mathcal{U}$.

The second inequality is equivalent to

$$\begin{aligned}L_{k+1} - L_k &= 1 - (1 - \alpha_k)^2 + \beta_k^2 - (\alpha_k + \beta_k) \\ &= (\alpha_k - \beta_k)(1 - (\alpha_k + \beta_k)) \leq 0\end{aligned}$$

which holds for all $(\alpha_k, \beta_k) \in \mathcal{U}$.

APPENDIX I
PROOF OF THEOREM 2

From Proposition 9, we have

$$L_1 = \widetilde{a} L_0^2$$

for some $\widetilde{a} \geq 1$. And, by Proposition 6, the following identity holds:

$$L_{k+2} = a_k L_k^2$$

for $k = 1, 3, \ldots, \log N - 2$ and some $a_k \in [1, 2]$. Hence, we can write

$$L_k = \widetilde{a}^{2^{(k-1)/2}} \cdot a_{(k-1)/2} \cdot a_{(k-3)/2}^2 \ldots a_1^{2^{(k-3)/2}} L_0^{2^{(k+1)/2}}$$

where $a_i \in [1, 2]$ for each i and $\widetilde{a} \geq 1$. Let $k = \log N$; we have

$$\begin{aligned}\log P_N^{-1} = &-2^{(k-1)/2} \log \widetilde{a} - \log a_{(k-1)/2} - \cdots \\ &- 2^{(k-3)/2} \log a_1 + \sqrt{2N} \log L_0^{-1}.\end{aligned}$$

Notice that $\log L_0^{-1} > 0$ and for each i, $\log a_i \geq 0$. Moreover, $\log \widetilde{a} \geq 0$. Hence

$$\log P_N^{-1} \leq \sqrt{2N} \log L_0^{-1}.$$

It follows by Proposition 9 that

$$L_k = \widetilde{a} L_{k-1}$$

for some $\widetilde{a} \in (0, 1]$. By Proposition 6, we have

$$L_{k+2} = a_k L_k^2$$

for $k = 0, 2, \ldots, \log N - 3$ and some $a_k \in [1, 2]$. Thus

$$L_k = \widetilde{a} \cdot a_{(k-3)/2} \cdot a_{(k-3)/2}^2 \ldots a_0^{2^{(k-3)/2}} L_0^{2^{(k-1)/2}}$$

where $a_i \in [1, 2]$ for each i and $\widetilde{a} \in (0, 1]$. Hence

$$\begin{aligned}\log P_N^{-1} = &- \log \widetilde{a} - \log a_{(k-1)/2} - \cdots \\ &- 2^{(k-3)/2} \log a_1 + \sqrt{\frac{N}{2}} \log L_0^{-1}.\end{aligned}$$

Notice that $\log L_0^{-1} > 0$ and for each i, $0 \leq \log a_i \leq 1$ and $\log \widetilde{a} \leq 0$. Thus,

$$\log P_N^{-1} \geq -\sqrt{\frac{N}{2}} + \sqrt{\frac{N}{2}} \log L_0^{-1} = \sqrt{\frac{N}{2}} \left(\log L_0^{-1} - 1 \right).$$

APPENDIX J
PROOF OF PROPOSITION 10

The upper bound for L_{k+1}/L_k is trivial. By Proposition 2, if $(\alpha_{k-1}, \beta_{k-1}) \in B_2 \cap R_{\mathcal{U}}$, then

$$1 \leq \frac{L_k}{L_{k-1}^2} \leq 2;$$

i.e.,

$$\frac{1}{2} \leq \frac{L_{k-1}^2}{L_k} \leq 1$$

and in consequence of Proposition 6, if $(\alpha_{k-1}, \beta_{k-1}) \in B_2 \cap R_{\mathcal{U}}$, then

$$1 \leq \frac{L_{k+1}}{L_{k-1}^2} \leq 2.$$

Therefore, we have

$$\frac{1}{2} \leq \frac{L_{k+1}}{L_k}.$$

APPENDIX K
PROOF OF THEOREM 3

If $(\alpha_m, \beta_m) \in B_2 \cap R_{\mathcal{U}}$ and m is even, then by Proposition 2, we have

$$L_{m+1} = \widetilde{a} L_m^2$$

for some $\widetilde{a} \in [1, 2]$.

By Proposition 6, we have

$$L_{k+2} = a_k L_k^2$$

for $k = 0, 2, \ldots, m-2, m+1, \ldots, \log N - 2$, and some $a_k \in [1, 2]$. Hence,

$$L_k = a_{(k-1)/2} \cdot a_{(k-3)/2}^2 \ldots a_0^{2^{(k-1)/2}} L_0^{2^{(k+1)/2}}$$

where $a_i \in [1, 2]$ for each i.

Let $k = \log N$; we have

$$\begin{aligned} \log P_N^{-1} = &- \log a_{(k-1)/2} - 2 \log a_{(k-3)/2} - \cdots \\ &- 2^{(k-1)/2} \log a_0 + \sqrt{2N} \log L_0^{-1}. \end{aligned}$$

Notice that $\log L_0^{-1} > 0$ and for each i, $0 \le \log a_i \le 1$. Thus

$$\log P_N^{-1} \le \sqrt{2N} \log L_0^{-1}.$$

Finally,

$$\log P_N^{-1} \ge -\sqrt{2N} + \sqrt{2N} \log L_0^{-1} = \sqrt{2N} \left(\log L_0^{-1} - 1 \right).$$

If $(\alpha_m, \beta_m) \in B_2 \cap R_{\mathcal{U}}$ and m is odd, then by Proposition 10 we have

$$L_{m+2} = \widetilde{a} L_{m+1}$$

for some $\widetilde{a} \in [1/2, 1]$.

It follows from Proposition 6 that

$$L_{k+2} = a_k L_k^2$$

for $k = 0, 2, \ldots, m-1, m+2, \ldots, \log N - 2$ and some $a_k \in [1, 2]$. Therefore

$$L_k = a_{(k-3)/2} \cdot a_{(k-3)/2}^2 \ldots a_0^{2^{(k-3)/2}} \cdot \widetilde{a}^{2^{(k-m-2)/2}} L_0^{2^{(k-1)/2}}$$

where $a_i \in [1, 2]$ for each i and $\widetilde{a} \in [1/2, 1]$. Hence

$$\begin{aligned} \log P_N^{-1} = &- \sqrt{\frac{N}{2^{m+2}}} \log \widetilde{a} - \log a_{(k-3)/2} - \cdots \\ &- \frac{\sqrt{N/2}}{2} \log a_0 + \sqrt{\frac{N}{2}} \log L_0^{-1}. \end{aligned}$$

Notice that $\log L_0^{-1} > 0$ and for each i, $0 \le \log a_i \le 1$ and $-1 \le \log \widetilde{a} \le 0$. Thus

$$\log P_N^{-1} \le \sqrt{\frac{N}{2}} \log L_0^{-1} + \sqrt{\frac{N}{2^{m+2}}}.$$

Finally

$$\log P_N^{-1} \ge -\sqrt{\frac{N}{2}} + \sqrt{\frac{N}{2}} \log L_0^{-1} = \sqrt{\frac{N}{2}} \left(\log L_0^{-1} - 1 \right).$$

APPENDIX L
PROOF OF THEOREM 4

If $\log N < m$, then this scenario is the same as that of Corollary 1. Therefore,

$$N \left(\log L_0^{-1} - 1 \right) \le \log P_N^{-1} \le N \log L_0^{-1}.$$

If $\log N \ge m$ and $\log N - m$ is odd, then it takes $(m-1)$ steps for the system to move into B_1. After it arrives in B_1, there is an even number of levels left because $\log N - m$ is odd.

By Proposition 2, we have

$$L_{k+1} = \widetilde{a}_k L_k^2$$

for $k = 0, 1, \ldots, m-2$ and some $\widetilde{a}_k \in [1, 2]$, and in consequence of Proposition 6

$$L_{k+2} = a_k L_k^2$$

for $k = m-1, m-3, \ldots, \log N - 2$ and some $a_k \in [1, 2]$. Thus

$$L_k = a_{(k+m-3)/2} \cdot a_{(k+m-5)/2}^2 \ldots a_0^{2^{(k+m-3)/2}} L_0^{2^{(k+m-1)/2}}$$

where $a_i \in [1, 2]$ for each i.

Let $k = \log N$. Then we obtain

$$\begin{aligned} \log P_N^{-1} = &- \log a_{(k+m-3)/2} - 2 \log a_{(k+m-5)/2} - \cdots \\ &- \frac{\sqrt{2^{m-1}N}}{2} \log a_0 + \sqrt{2^{m-1}N} \log L_0^{-1}. \end{aligned}$$

Note that $\log L_0^{-1} > 0$, and for each i, $0 \le \log a_i \le 1$. Thus,

$$\log P_N^{-1} \le \sqrt{2^{m-1}N} \log L_0^{-1}.$$

Finally,

$$\begin{aligned} \log P_N^{-1} &\ge -\sqrt{2^{m-1}N} + \sqrt{2^{m-1}N} \log L_0^{-1} \\ &= \sqrt{2^{m-1}N} \left(\log L_0^{-1} - 1 \right). \end{aligned}$$

For the case where $\log N - m$ is even, the proof is similar and it is omitted.

APPENDIX M
PROOF OF PROPOSITION 11

Without loss of generality, we consider the upper half of S, denoted by $S_{\mathcal{U}}$. As we shall see, the image of $S_{\mathcal{U}}$ is exactly the reflection of $S_{\mathcal{U}}$ with respect to the line $\beta = \alpha$ (denoted by $S_{\mathcal{L}}$). We know that $S_{\mathcal{U}} := \{(\alpha, \beta) \in \mathcal{U} | \beta \le \sqrt{\alpha}$ and $\beta \ge 1 - (1-\alpha)^2\}$.

The image of $S_{\mathcal{U}}$ under f can be calculated by

$$(\alpha', \beta') = f(\alpha, \beta) = (1 - (1-\alpha)^2, \beta^2)$$

where $(\alpha, \beta) \in \mathcal{U}$. The aforementioned relation is equivalent to

$$(\alpha, \beta) = (1 - \sqrt{1 - \alpha'}, \sqrt{\beta'}).$$

Therefore, we can calculate images of boundaries for $R_{\mathcal{U}}$ under f.

The image of the upper boundary $\beta \leq \sqrt{\alpha}$ is

$$\sqrt{\beta'} \leq \sqrt{1-\sqrt{1-\alpha'}};$$

i.e.,

$$\alpha' \geq 1-(1-\beta')^2$$

and that of the lower boundary $\beta \geq 1-(1-\alpha)^2$ is

$$\sqrt{\beta'} \geq 1-(1-(1-\sqrt{1-\alpha'}))^2;$$

i.e.,

$$\alpha' \leq \sqrt{\beta'}.$$

The function f is monotone. Hence, images of boundaries of $S_{\mathcal{U}}$ are boundaries of $S_{\mathcal{L}}$. Notice that boundaries of $R_{\mathcal{L}}$ are symmetric with those of $R_{\mathcal{U}}$ about $\beta=\alpha$. We conclude that S is an invariant region.

ACKNOWLEDGMENT

The authors wish to thank the anonymous reviewers and associate editor for the careful reading of the manuscript and constructive comments that have improved the presentation.

REFERENCES

[1] R. R. Tenney and N. R. Sandell, "Detection with distributed sensors," *IEEE Trans. Aerosp. Electron. Syst.*, vol. AES-17, no. 4, pp. 501–510, Jul. 1981.

[2] Z. Chair and P. K. Varshney, "Optimal data fusion in multiple sensor detection systems," *IEEE Trans. Aerosp. Electron. Syst.*, vol. AES-22, no. 1, pp. 98–101, Jan. 1986.

[3] J.-F. Chamberland and V. V. Veeravalli, "Asymptotic results for decentralized detection in power constrained wireless sensor networks," *IEEE J. Sel. Areas Commun.*, vol. 22, no. 6, pp. 1007–1015, Aug. 2004.

[4] J. N. Tsitsiklis, "Decentralized detection," *Adv. Statist. Signal Process.*, vol. 2, pp. 297–344, 1993.

[5] G. Polychronopoulos and J. N. Tsitsiklis, "Explicit solutions for some simple decentralized detection problems," *IEEE Trans. Aerosp. Electron. Syst.*, vol. 26, no. 2, pp. 282–292, Mar. 1990.

[6] W. P. Tay, J. N. Tsitsiklis, and M. Z. Win, "Asymptotic performance of a censoring sensor network," *IEEE Trans. Inf. Theory*, vol. 53, no. 11, pp. 4191–4209, Nov. 2007.

[7] P. Willett and D. Warren, "The suboptimality of randomized tests in distributed and quantized detection systems," *IEEE Trans. Inf. Theory*, vol. 38, no. 2, pp. 355–361, Mar. 1992.

[8] R. Viswanathan and P. K. Varshney, "Distributed detection with multiple sensors: Part I—Fundamentals," *Proc. IEEE*, vol. 85, no. 1, pp. 54–63, Jan. 1997.

[9] R. S. Blum, S. A. Kassam, and H. V. Poor, "Distributed detection with multiple sensors: Part II—Advanced topics," *Proc. IEEE*, vol. 85, no. 1, pp. 64–79, Jan. 1997.

[10] T. M. Duman and M. Salehi, "Decentralized detection over multiple-access channels," *IEEE Trans. Aerosp. Electron. Syst.*, vol. 34, no. 2, pp. 469–476, Apr. 1998.

[11] B. Chen and P. K. Willett, "On the optimality of the likelihood-ratio test for local sensor decision rules in the presence of nonideal channels," *IEEE Trans. Inf. Theory*, vol. 51, no. 2, pp. 693–699, Feb. 2005.

[12] B. Liu and B. Chen, "Channel-optimized quantizers for decentralized detection in sensor networks," *IEEE Trans. Inf. Theory*, vol. 52, no. 7, pp. 3349–3358, Jul. 2006.

[13] B. Chen and P. K. Varshney, "A Bayesian sampling approach to decision fusion using hierarchical models," *IEEE Trans. Signal Process.*, vol. 50, no. 8, pp. 1809–1818, Aug. 2002.

[14] A. Kashyap, "Comments on on the optimality of the Likelihood-Ratio test for local sensor decision rules in the presence of nonideal channels," *IEEE Trans. Inf. Theory*, vol. 52, no. 3, pp. 1274–1275, Mar. 2006.

[15] H. Chen, B. Chen, and P. K. Varshney, "Further results on the optimality of the likelihood-ratio test for local sensor decision rules in the presence of nonideal channels," *IEEE Trans. Inf. Theory*, vol. 55, no. 2, pp. 828–832, Feb. 2009.

[16] G. Fellouris and G. V. Moustakides, "Decentralized sequential hypothesis testing using asynchronous communication," *IEEE Trans. Inf. Theory*, vol. 57, no. 1, pp. 534–548, Jan. 2011.

[17] J. A. Gubner, L. L. Scharf, and E. K. P. Chong, "Exponential error bounds for binary detection using arbitrary binary sensors and an all-purpose fusion rule in wireless sensor networks," in *Proc. IEEE Int. Conf. Acoustics, Speech, Signal Process*, Taipei, Taiwan, Apr. 19–24, 2009, pp. 2781–2784.

[18] Z. B. Tang, K. R. Pattipati, and D. L. Kleinman, "Optimization of detection networks: Part I—Tandem structures," *IEEE Trans. Syst., Man, Cybern.*, vol. 21, no. 5, pp. 1044–1059, Sep./Oct. 1991.

[19] R. Viswanathan, S. C. A. Thomopoulos, and R. Tumuluri, "Optimal serial distributed decision fusion," *IEEE Trans. Aerosp. Electron. Syst.*, vol. 24, no. 4, pp. 366–376, Jul. 1988.

[20] W. P. Tay, J. N. Tsitsiklis, and M. Z. Win, "On the sub-exponential decay of detection error probabilities in long tandems," *IEEE Trans. Inf. Theory*, vol. 54, no. 10, pp. 4767–4771, Oct. 2008.

[21] J. D. Papastravrou and M. Athans, "Distributed detection by a large team of sensors in tandem," *IEEE Trans. Aerosp. Electron. Syst.*, vol. 28, no. 3, pp. 639–653, Jul. 1992.

[22] V. V. Veeravalli, "Topics in Decentralized Detection," Ph.D. dissertation, Univ. Illinois, Urbana-Champaign, 1992.

[23] Z. B. Tang, K. R. Pattipati, and D. L. Kleinman, "Optimization of detection networks: Part II—Tree structures," *IEEE Trans. Syst., Man, Cybern.*, vol. 23, no. 1, pp. 211–221, Jan./Feb. 1993.

[24] W. P. Tay, J. N. Tsitsiklis, and M. Z. Win, "Data fusion trees for detection," *IEEE Trans. Inf. Theory*, vol. 54, no. 9, pp. 4155–4168, Sep. 2008.

[25] A. R. Reibman and L. W. Nolte, "Design and performance comparison of distributed detection networks," *IEEE Trans. Aerosp. Electron. Syst.*, vol. AES-23, no. 6, pp. 789–797, Nov. 1987.

[26] W. P. Tay and J. N. Tsitsiklis, "Error exponents for decentralized detection in tree networks," in *Networked Sensing Information and Control*, V. Saligrama, Ed. New York: Springer-Verlag, 2008, pp. 73–92.

[27] W. P. Tay, J. N. Tsitsiklis, and M. Z. Win, "Bayesian detection in bounded height tree networks," *IEEE Trans. Signal Process*, vol. 57, no. 10, pp. 4042–4051, Oct. 2009.

[28] A. Pete, K. R. Pattipati, and D. L. Kleinman, "Optimization of detection networks with multiple event structures," *IEEE Trans. Autom. Control*, vol. 39, no. 8, pp. 1702–1707, Aug. 1994.

[29] O. P. Kreidl and A. S. Willsky, "An efficient message-passing algorithm for optimizing decentralized detection networks," *IEEE Trans. Autom. Control*, vol. 55, no. 3, pp. 563–578, Mar. 2010.

[30] S. Alhakeem and P. K. Varshney, "A unified approach to the design of decentralized detection systems," *IEEE Trans. Aerosp. Electron. Syst.*, vol. 31, no. 1, pp. 9–20, Jan. 1995.

[31] Y. Lin, B. Chen, and P. K. Varshney, "Decision fusion rules in multi-hop wireless sensor networks," *IEEE Trans. Aerosp. Electron. Syst.*, vol. 41, no. 2, pp. 475–488, Apr. 2005.

[32] J. A. Gubner, E. K. P. Chong, and L. L. Scharf, "Aggregation and compression of distributed binary decisions in a wireless sensor network," in *Proc. Joint 48th IEEE Conf. Decision and Control and 28th Chinese Control Conf.*, Shanghai, China, Dec. 16–18, 2009, pp. 909–913.

[33] P. K. Varshney, *Distributed Detection and Data Fusion*. New York: Springer-Verlag, 1997.

[34] H. L. Van Trees, *Detection, Estimation, and Modulation Theory, Part I*. New York: Wiley, 1968.

Zhenliang Zhang (S'09) received the B.S. degree in physics from Special Class for Gifted Young, University of Science and Technology of China, Hefei, China, in 2008.

He is currently working toward the Ph.D. degree in the Department of Electrical and Computer Engineering, Colorado State University, CO. His research interests include distributed detection, hierarchical system, and applications of POMDP in sensor networks.

Ali Pezeshki (S'95–M'05) received the B.Sc. and M.Sc. degrees in electrical engineering from the University of Tehran, Tehran, Iran, in 1999 and 2001, respectively. He received the Ph.D. degree in electrical engineering from Colorado State University in 2004. In 2005, he was a postdoctoral research associate with the Electrical and Computer Engineering Department at Colorado State University. From January 2006 to August 2008, he was a postdoctoral research associate with The Program in Applied and Computational Mathematics at Princeton University. Since August 2008, he has been an assistant professor with the Department of Electrical and Computer Engineering, Colorado State University, Fort Collins. His research interests are in statistical signal processing and coding theory and their applications to active/passive sensing.

William Moran (M'95) received the B.S. (Hons.) degree in mathematics from the University of Birmingham in 1965 and the Ph.D. degree in mathematics from the University of Sheffield, London, U.K., in 1968. He is currently a Professor of electrical engineering with the University of Melbourne, Australia, where he is the Research Director of Defence Science Institute and Technical Director of Melbourne Systems Laboratory. Previously, he was a Professor of mathematics with the University of Adelaide and Flinders University. He also serves as a Consultant to the Australian Department of Defence through the Defence Science and Technology Organization. His research interests are in signal processing, particularly with radar applications, waveform design and radar theory, and sensor management. He also works in various areas of mathematics, including harmonic analysis and number theory and has published widely in these areas.

Stephen D. Howard (M'09) graduated in 1982 from La Trobe University, Melbourne, Australia. He received the M.S. and Ph.D. degrees in mathematics from La Trobe University in 1984 and 1990, respectively. He joined the Australian Defence Science and Technology Organisation (DSTO) in 1991, where he has been involved in research in the area electronic surveillance and radar systems. He has led the DSTO research effort into the development of algorithms in all areas of electronic surveillance, including radar pulse train deinterleaving, precision radar parameter estimation and tracking, estimation of radar intrapulse modulation, and advanced geolocation techniques. Since 2003, he has led the DSTO long-range research program in radar resource management and waveform design. He is currently the recipient of a three-year DSTO research fellowship.

Edwin K. P. Chong (F'04) received the B.E. degree with First Class Honors from the University of Adelaide, South Australia, in 1987; and the M.A. and Ph.D. degrees in 1989 and 1991, respectively, both from Princeton University, where he held an IBM Fellowship. He joined the School of Electrical and Computer Engineering at Purdue University in 1991, where he was named a University Faculty Scholar in 1999. Since August 2001, he has been a Professor of Electrical and Computer Engineering and Professor of Mathematics at Colorado State University. His current research interests span the areas of stochastic modeling and control, optimization methods, and communication and sensor networks. He coauthored the best-selling book *An Introduction to Optimization* (3rd Edition, Wiley-Interscience, 2008). He received the NSF CAREER Award in 1995 and the ASEE Frederick Emmons Terman Award in 1998. He was a corecipient of the 2004 Best Paper Award for a paper in the journal *Computer Networks*. In 2010, he received the IEEE Control Systems Society Distinguished Member Award.

Prof. Chong was the founding chairman of the IEEE Control Systems Society Technical Committee on Discrete Event Systems, and served as an IEEE Control Systems Society Distinguished Lecturer. He is currently a Senior Editor of the IEEE TRANSACTIONS ON AUTOMATIC CONTROL, and also serves on the editorial boards of *Computer Networks*, the international journal of control science and engineering, and IEEE Expert Now. He is a member of the IEEE Control Systems Society Board of Governors (2006–2008, 2010–present). He has also served on the organizing committees of several international conferences. He has been on the program committees for the IEEE Conference on Decision and Control, the American Control Conference, the IEEE International Symposium on Intelligent Control, IEEE Symposium on Computers and Communications, and the IEEE Global Telecommunications Conference. He has also served in the executive committees for the IEEE Conference on Decision and Control, the American Control Conference, the IEEE Annual Computer Communications Workshop, the International Conference on Industrial Electronics, Technology & Automation, and the IEEE International Conference on Communications. He was the Conference (General) Chair for the Conference on Modeling and Design of Wireless Networks, part of SPIE ITCom 2001. He was the General Chair for the 2011 Joint 50th IEEE Conference on Decision and Control and European Control Conference.